TECHNICAL PAPER

Experimental investigation and optimization of process stability in drilling of Al 7075-T651 using indexable insert drills

Aslan Akdulum[1] · Yunus Kayir[2]

Abstract

The indexable insert drill, commonly known as the U drill, holds a significant market share of approximately 53% among drilling tools. Therefore, investigation and improvement studies are carried out by both industry and academia. U drills are usually produced in different length/diameter ratios and with two coolant holes. But in other cases, some manufacturers design a third coolant hole in the chip evacuation channel, where the central insert of the U drills is located. It is thought that the coolant holes and length/diameter ratios change the conditions of the drilling process. In this study, the impact of U drills with various attributes was examined using thrust force, torque, spindle load, and audio signals. For this purpose, Al 7075-T651 aluminum alloy was drilled with 4 different U drills. The trials used three feed rates (0.06, 0.09, and 0.12 mm/rev) and three cutting speeds (200, 250, and 300 m/min). Experimental results show that the length/diameter ratio of U drills has the highest impact on thrust force (76.45%), spindle load (53.33%), and audio signal (87.53%). However, it was ineffective for torque, according to the Anova analysis. Moreover, the U drill, which has an additional coolant hole, generates higher thrust forces (39.89%) and audio signals (95.17%), lower spindle loads (41.28%), and lower torque (3.26%). Taguchi based grey relational analysis that was used to optimize the test parameters provided an improvement of 26.06% according to the gray relationship grade, which is the normal method used. To sum up, these findings may contribute to improving the design and production of U drills to enhance their drilling performance.

Keywords Al 7075-T651 · U drill · Spindle load · Thrust force · Torque · Audio signal

1 Introduction

7075 aluminum alloy is one of the most preferred materials in aerospace [1]. And, to enhance the alloy's mechanical qualities, some hardening procedures, such as T651 precipitation, are applied [2]. 7075 aluminum alloy, to which this process is applied, is used extensively in various industries such as aviation and automotive due to its low density and good mechanical properties [3, 4]. Drilling operations have

an important place in many sectors and are also where this material is used [5]. It is estimated that the rate of drilling in total metal cutting operations is 36% when all machines are taken into account. This rate is approximately 40% for CNC machines, 25% for turning, and 26% for milling [6]. As drilling is done in a partially enclosed space, some problems may occur, for example, friction between the tool and the workpiece, high drilling temperatures, and challenges with chip removal [7]. The cut chips adhere to the cutting edges and chip evacuation channels of the drills used to drill aluminum materials. Thus, chip evacuation becomes difficult. This situation negatively affects the drilling process by causing the thrust force, torque, and spindle load to increase more than necessary. In addition, chips adhering to the drill cause the hole quality to deteriorate as they contact the hole simultaneously. Numerous experiments are conducted by altering the angles, coatings, and cutting parameters in drilling operations to remove these negative effects. Table 1 lists a few of these studies on drilling the alloy Al 7075.

Technical Editor: Adriano Fagali de Souza.

✉ Aslan Akdulum
a.akdulum@gmail.com.tr

Yunus Kayir
ykayir@gazi.edu.tr

[1] Department of Manufacturing Engineering, Gazi University, Ankara, Turkey

[2] Department of Manufacturing Engineering, Faculty of Technology, Gazi University, Ankara, Turkey

Table 1 An overview of many investigations on drilling Al 7075 alloy

Material	Drill	Cutting factors	Responses	References
7075-T6	$D = 10$ mm Dq = Wolfram carbide (WC)	$f = 60, 100, 140$ mm/min SS = 800, 1000, 1200 rpm	Fz, Mz, T, TW, CG	[7]
7075	$D = 15$ mm Dq = HSS	$f = 0.13, 0.18, 0.25$ mm/rev Vc = 8, 14, 20 m/min PA = 100, 118, 135°	Cy, Ce, SR, Fz, CG	[8]
7075-T6	D = 2.4 and 3 mm Dq = HSS	SS = 1000, 4000 rpm $f = 40, 60, 90, 150, 200$ mm/min VA = 0.002, 0.0035 mm VF = 100, 200, 1000 Hz	BH, Fz	[5]
7075	$D = 5$ mm Dq = WC (Uncoated, TiAlN coated, Diamond Coated)	f = 0.05, 0.1, 0.15 mm/rev Vc = 40, 80, 120 m/min PA = 120, 130, 140°	Fz, SR	[3]
7075	$D = 4, 5, 6$ mm Dq = HSS (TiN Coated, TiAlN Coated)	PA = 118, 126, 135° SS = 910, 1420, 2000 rpm $f = 0.06, 0.08, 0.1$ mm/rev	DE, TW, SR, Ce	[9]
7075	$D = 5$ mm Dq = HSS	SS = 1000, 1250, 1500 rpm $f = 100, 150, 200$ mm/min	Ce, TW, CG	[4]
7075-T6	Dq = HSS	SS = 250, 355, 500, 710, 1000 rpm $f = 0.08, 0.11, 0.14, 0.2$ mm/rev	Fz, Mz	[10]
7075-T6	$D = 8$ mm Dq = WC–Co (Twist drill and 3-flute drills)	$f = 0.05, 0.1, 0.2$ mm/rev Vc = 60, 90, 120, 150 m/min	Fz, Mz	[11]
7075-T651	$D = 10$ mm Dq = TiN/TiAlN- coated carbide drills	SS = 1910, 2547, 3184 rpm $f = 0.1, 0.15, 0.2$ mm/rev DD = 20, 30, 40 mm	T, Fz	[12]

Fz Thrust Force, *Mz* Torque, *T* Temperature, *TW* Tool Wear, *CG* Chip Geometry, *Cy* Cylindricity, *Ce* Circularity, *SR* Surface roughness, *PA* Point Angle, *VA* Vibration amplitude, *VF* Vibration frequency, *BH* Burr Height, *Dq* Drill quality, *DE* Diametrical error, *DD* Drilling Depth

When the list is carefully examined, normal helical drills are generally preferred for drilling Al 7075 alloy. However, when the diameter of drills increases to drill larger holes, higher thrust forces occur due to the enlargement of the chisel edge in normal helical drills [8, 9]. Larger-diameter drills also have longer contact times with the workpiece. With the increased contact length, more workpiece material rubs and sticks to the cutting edges, margin, and chip evacuation channel. Due to the increased adhesion of more material to the cutter and the hole wall, the thrust force, torque, and spindle load are unusually increased. Furthermore, this results in increased energy consumption and the failure of the drilling operation. Even in some cases, the cutting edges and margins of the drill may become unusable due to the effect of adhering aluminum materials. In order to prevent this situation, peck drilling is performed. When the hole diameter increases too much, pre-drilling operations are required. This means extra time and costs in manufacturing. Alternatively, U drills with indexable inserts, without margin, and with a shorter contact length are used to overcome these disadvantages when drilling holes with a diameter larger than 12. It is stated that U drills have a market share of 53% in drilling tools and 8% in the total cutting tool sector [13]. However, there are very few studies on drilling holes using the U drill. When the studies using U drills are

examined, steel materials are generally used as workpieces. These studies looked at how drilling parameters affected forces, surface quality, drill wear, vibration, and hole size, and they found that U drills generated higher-quality holes than standard helical drills [14, 15]. It has been found that using different geometry inserts has an effect on output parameters such as thrust force, torque, and surface roughness [16, 17]. Mathematical models are used to examine the impact of yield strength, forces, and cutting edge geometry on burr development [18]. The cutter wear, thrust force, torque, and surface quality of several cooling techniques, including dry, compressed air, emulsion, and MQL, were studied. It was discovered that emulsion cooling produced the least thrust force and surface roughness [19]. Compared to wet cooling, cryogenic liquid nitrogen (LN_2) cooling has been found to reduce temperature, thrust, torque, surface roughness, and deviation from circularity and cylindricality [20]. Cylindricality and perpendicularity were estimated and optimized by gray relational analysis [21]. Investigating the effects of various insert coatings on thrust force, torque, and hole quality led to the conclusion that coating is a crucial factor [22, 23]. In a developed tool condition monitoring system using the current of spindle and axial feed motors, wear and hole diameter estimation have been made successfully [24]. Examining torsion, lateral regeneration chatter,

and whirling in vibration and sound measurement findings led to the effective development of a mechanistic model [25, 26]. A specially made U drill was designed with an axially placed heat pipe. It has been determined that the heat pipes reduce the cutting temperature compared to dry machining [27]. The thrust force, torque, and temperature distribution of U drills were modeled using the finite element method. When the experimental and model data were compared, the torque was effectively modeled, but the anticipated thrust force had an inaccuracy of between 12 and 20 percent [28]. According to the studies in which steel group materials are drilled, different output responses are obtained due to the different mechanical and dynamic structures of the U drill and the normal helical drill. Therefore, further research on U drills and their effects on materials from different groups is required.

When the studies in the literature in which aluminum alloys were drilled with U drills were examined, a few and insufficient studies could be found. While drilling AlCuMgPb-F34 alloy with a U drill, it was determined that the burr value decreased to almost zero with the minimum amount of lubrication compared to dry machining [29]. Under carbon dioxide snow jet and emulsion machining conditions, AlMgSi1 alloy was compared in terms of burr height, surface roughness, diameter, and deviation from circularity. It has been indicated that the cooling methods are ineffective in reducing the deviation from the diameter and circularity of the holes in this material. But, it should not be drilled in dry conditions due to the high adhesion of aluminum to the cutter [30]. In some drilling, Al 7050-T7451 material is also mathematically modeled. The estimated thrust force and lateral force were compatible with the experimental result after the pre-drilling [31]. But for the Al 7075 material, an error of 38% in lateral forces and 60% in thrust forces occurred between the experimental results obtained from the pre-drilling and the estimation results. According to some reports, the U drill's low center cutting speed and the side edge of the central insert's close proximity to this area are to blame for the high mistake rates [32]. When the studies in which aluminum alloys are drilled with U drills are examined, a very insufficient amount of research has been done. Further studies need to be investigated by drilling aluminum alloys with U drills. Because the U drill has very different mechanical and dynamic properties from a normal twist drill. Actually, the U drill is a drill with two indexable inserts, one in the center and one on the periphery [16]. The central insert is the first to come into contact with the material and is responsible for centering the U drill. The peripheral insert provides that hole quality, which is achieved by cutting the part between the central insert and the hole diameter. Since the inserts are positioned at different distances from the U drill center, different insert geometry, grade, and balance angle can be used to balance the radial forces [25]. In addition, the chip evacuation channels designed for each insert have different

geometric properties [13]. Due to the mentioned mechanical properties of the U drill, mathematical modeling and modeling with the finite element method led to high false force estimates (12–60%). It is important to make estimates that approximate experimental results by using different modeling techniques. Therefore, it is necessary to model and optimize the input parameters by experimentally examining the output responses such as thrust force, torque, and spindle load. The Taguchi-based gray relational analysis approach is one of the techniques used for modeling and optimization. The best experimentation sequence is chosen using this multi-criteria decision-making process based on all output replies. The optimal input parameters and percentage contributions are determined by the main effects plot and response tables. As a result, output responses are estimated and experimentally verified according to the most optimal input parameters. This method has been used efficiently in various studies. For example, optimization of cutting force, temperature, and surface roughness obtained from experiments with cooling method, feed rate, and cutting speed input parameters has been carried out [33]. In a different investigation, the input parameters of the drill type, feed rate, and cutting speed were used to optimize the thrust force, temperature, and burr height [34]. The goal of optimization is to choose the proper drilling parameters. Thus, it will be possible to increase hole quality, achieve optimum drilling forces, and have a more efficient drilling process [6]. Monitoring the drilling process involves using a variety of techniques or output responses. A dynamometer can be used to measure the thrust and torque data used to track the drilling process in real time. There is a correlation between the thrust force and torque signals, the surface delamination, and the surface integrity of the drilled hole, according to research employing standard helical drills [35, 36]. The relationship between the thrust force and vibration signals has been established, and the thrust force signals can be used to monitor the tool status [37, 38]. The relationship between the thrust force and torque values and the feed rate and cutting speed has been established [39]. Therefore, while analyzing output reactions like thrust force and torque, feed rate and cutting speed should be taken into consideration as input variables. A comparison of U drills with different properties apart from the mentioned input parameters is important in terms of production efficiency. In general, U drills have two cooling holes for in-hole cooling [14]. The manufacturer drills a third cooling hole even though some have the same length to diameter ratio because they believe the coolant will penetrate the cutting media more deeply. However, since the effect of this third cooling hole on the cutting process has not been examined before, it is a matter of curiosity and a gap in the literature. The cutting process dynamics may become unstable as a result of variations on the U drill body [17]. The additional coolant hole can alter the U drill's dynamic behavior by adding extra space to the body. Rigidities on the body can cause the drill to rotate backward,

causing instantaneous elongation and shortening, resulting in vibrations [25]. Vibrations can cause unbalanced forces and adversely affect the cutting process [40]. Unstable thrust forces and torque values can cause inefficient use of machine power, premature wear of cutters, worsening of hole quality, and noises that are harmful to human health in the working environment [41, 42]. Due to the low frequency range of the dynamometer, some vibration mechanisms obtained with the U drill cannot be detected during the drilling process. In addition to thrust force, torque, and spindle load, audio signals from the drilling environment can be used with a microphone can be used in real time to examine the drilling process in more detail. Because it has been stated that it is more useful to examine sound signals in order to detect high frequency levels [43]. It is also possible to control the instantaneous strain of the spindle due to the variable torque with the spindle load during the drilling process [44, 45]. Further research in this area could lead to the development of more effective drilling tools for aluminum materials, which would enhance manufacturing processes and reduce production costs.

The aim of the current study is to optimize the effect of machining parameters on thrust force, torque, spindle load, and audio signals, which occur when drilling Al 7075-T651 material with U drills with different properties, by modeling with Taguchi-based gray relational analysis, one of the multi-criteria decision making methods. Additionally, the analysis of the impact of the additional cooling hole is the study's major contribution to the literature. A standard U drill with the same nominal diameter and the same length/diameter ratio will be used to experimentally compare the effects on the output responses of the third extra coolant hole drilled by the U drill manufacturer. So, in this paper, the effects of the length/diameter ratio of the U drills, as well as the effect of the extra coolant hole, on the output responses were compared. The influence of mechanical changes between U drills on dynamic thrust force, torque, spindle load, and audio signals was investigated. For modeling and optimization of output responses, a Taguchi-based gray relational analysis method was applied. Thus, optimal input parameters were determined. The information obtained can be useful in the research and product development stages of U drills, as well as in increasing the quality of the drilled parts and the drilling efficiency.

2 Materials and methods

2.1 Experimental material

Al 7075-T651 aluminum alloy was used for the experimental studies. The workpiece has dimensions of $40 \times 40 \times 40$ mm. Hardness measurements and spectrum analysis were measured with at least three replications and averaged. The average hardness of the Al 7075-T651 material was determined at 172 Brinell. Table 2 shows the chemical composition of the material based on the spectrum analysis.

2.2 Machine tool used in experiments

In the experiments, a CNC milling machine tool named the Johnford VMC-850 was used. The machine has a spindle power of 7.5 KW, a maximum spindle speed of 8000 rpm, a measuring accuracy of 0.001 mm, and a Fanuc operating system. For the cooling process, the emulsion mixture was prepared with 5% semi-synthetic cutting fluid and water. The current investigation was carried out in accordance with the flow chart depicted in Fig. 1. Drilling tests were performed using the principles of through-hole and normal-hole drilling. The coolant was sprayed from the exterior and in one direction, as in the experimental configuration depicted in Fig. 2.

2.3 Cutting tool and cutting parameters

U drills with different length/diameter ratios (LD) (see Fig. 3) were used in the experiments. Totally, three different lengths of the U drill, such as 3D, 4D, and 5D, were preferred for experimental works. But tests were conducted for four types of the U drill. The fourth U drill is 4De, which has an extra cooling hole in the center. In Table 3, the size information of the U drills used in the experiments is given.

In Fig. 4, there is dimension information for the used inserts. Typically, no two inserts are the same; both edge geometry and coating might change as they work at varying cutting rates and under varying load situations.

The geometric parameters of the central and peripheral inserts of the U drill in this study differ, although both are uncoated carbide inserts appropriate for aluminum machining. XOET-ND 07T205 geometry was used as the central insert, and SPET-ND 07T208 geometry was used as the peripheral insert. Both inserts are of H01 quality. U drills of the same nominal diameter and inserts with the same specifications were used. A BT-40 VT-25 90 Veldon type tool holder was

Table 2 Al 7075-T651 aluminum alloy chemical composition,% by weight	Fe	Si	Mn	Cr	Ti	Cu	Mg	Zn	Al
	0,18	0,11	0,08	0,2	0,03	1,7	2,6	5,6	89,5

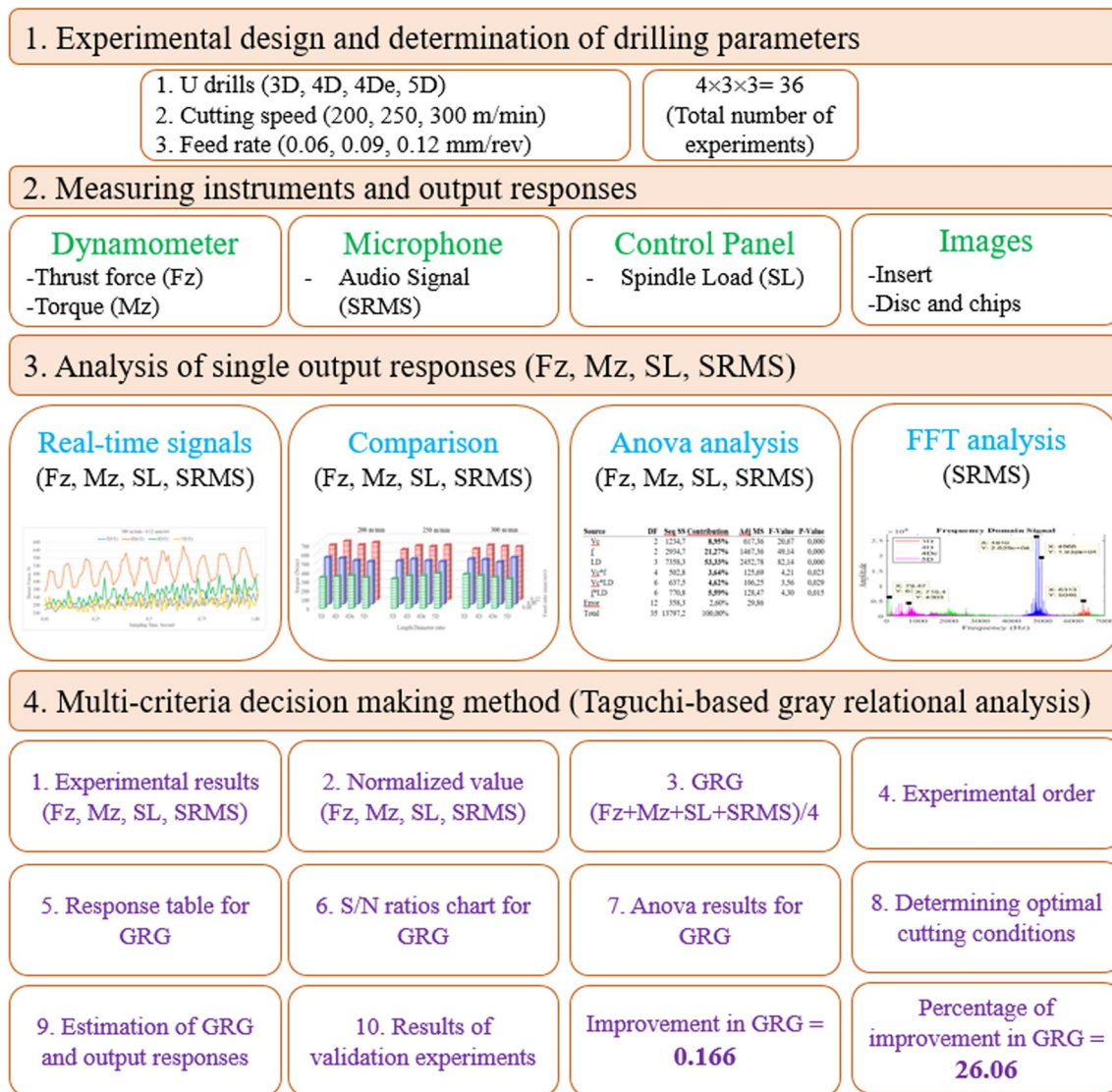**1. Experimental design and determination of drilling parameters**

1. U drills (3D, 4D, 4De, 5D)
2. Cutting speed (200, 250, 300 m/min)
3. Feed rate (0.06, 0.09, 0.12 mm/rev)

4×3×3= 36
(Total number of experiments)

2. Measuring instruments and output responses

Dynamometer
-Thrust force (Fz)
-Torque (Mz)

Microphone
- Audio Signal (SRMS)

Control Panel
- Spindle Load (SL)

Images
-Insert
-Disc and chips

3. Analysis of single output responses (Fz, Mz, SL, SRMS)

Real-time signals (Fz, Mz, SL, SRMS)

Comparison (Fz, Mz, SL, SRMS)

Anova analysis (Fz, Mz, SL, SRMS)

FFT analysis (SRMS)

4. Multi-criteria decision making method (Taguchi-based gray relational analysis)

1. Experimental results (Fz, Mz, SL, SRMS)

2. Normalized value (Fz, Mz, SL, SRMS)

3. GRG (Fz+Mz+SL+SRMS)/4

4. Experimental order

5. Response table for GRG

6. S/N ratios chart for GRG

7. Anova results for GRG

8. Determining optimal cutting conditions

9. Estimation of GRG and output responses

10. Results of validation experiments

Improvement in GRG = **0.166**

Percentage of improvement in GRG = **26.06**

Fig. 1 Process steps of the experimental study
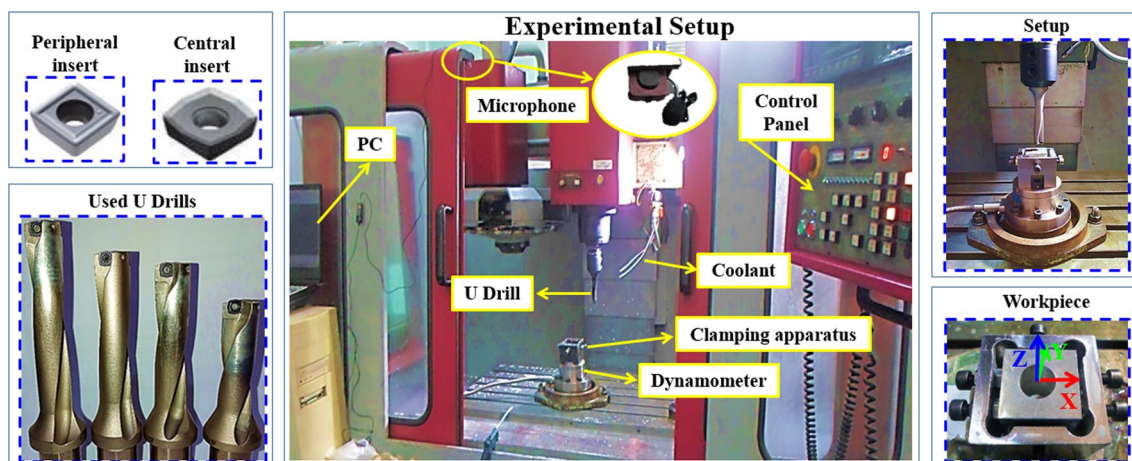
Fig. 2 The experimental setup

Fig. 3 U drills used in experiments

Table 3 U drill dimensions used

U drill	Diameter (*D*: mm)	Length (*L*: mm)
3D	20	60
4D, 4De		80
5D		100

used to connect the U drill to the spindle. While determining the drilling parameters, the cutting tool catalog recommendations and literature information were taken into account. Table 4 lists the drilling variables.

Fz and Mz forces were measured using a Kistler 9272 dynamometer. Kistler's 5070A was used as an amplifier. The samples were obtained at a rate of 100 Hz. The measured force and torque values, as well as the average numerical values, were obtained using the dynamometer's proprietary software, DynoWare. Spindle load values are taken from the control panel of the machine. The audio levels were taken from the cutting environment with the help of a LYM-333 microphone and recorded on the computer. The sampling amount of the audio signals was chosen as 44,100 Hz. The microphone position is fixed for all drilling experiments. All machines except the working CNC machine tool were turned off, and the audio signals were recorded by performing the experiments at a time when the ambient sound was minimal. The received audio

Table 4 Drilling variables used in the experiments

U drill length/diameter ratio (LD)	Feed rate, *f* (mm/rev)	Cutting speed, Vc (m/min)
3D	0.06	200
4D	0.09	250
4De		
5D	0.12	300

signals were normalized, and then their root mean square (RMS) was taken to obtain the final experimental results.

2.4 Grey relational analysis

The optimal result of each output response may be different from each other. Thus, the selection of optimal drilling parameters becomes difficult. Multi criteria decision-making methods are used to overcome such problems [21]. One of these methods is grey relational analysis. It is widely used in studies published recently. In this study, Al 7075-T651 alloy was drilled with U drills with different LD ratios. A Taguchi-based grey relational analysis approach was utilized to identify the optimal drilling variables by multi-response optimization of the drilling process's thrust force, torque, spindle load, and audio signal outputs.

3 Experimental results and discussion

A total of 36 experiments ($4 \times 3 \times 3$) were carried out in order to investigate the thrust force (Fz), torque (Mz), spindle load (SL), and RMS value of the audio signal (SRMS) in relation to the drilling variables. The repeatability of randomized experiments is over 98%. Table 5 contains the test results.

3.1 Evaluation of thrust force

Fz happens when the cutting tool enters the workpiece during drilling. In regular twist drills, the chisel edge is in charge of the most Fz, whereas in U drills, the central insert is in charge. Fz may result in excessive power consumption
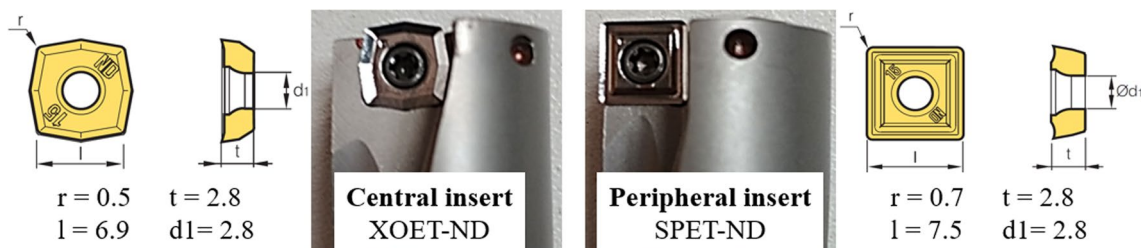

Fig. 4 Inserts and sizes

Table 5 Experimental results

Test number	Vc (m/min)	F (mm/rev)	LD	Fz (N)	Mz (Ncm)	SL (%)	SRMS (Pa)
1	200	0.06	3D	295	345	50	0.057
2	200	0.09	3D	329	517	60	0.054
3	200	0.12	3D	372	608	70	0.046
4	250	0.06	3D	275	328	60	0.056
5	250	0.09	3D	326	479	70	0.051
6	250	0.12	3D	371	558	75	0.040
7	300	0.06	3D	305	380	55	0.050
8	300	0.09	3D	333	500	90	0.052
9	300	0.12	3D	340	566	95	0.045
10	200	0.06	4De	478	364	55	0.168
11	200	0.09	4De	514	483	45	0.152
12	200	0.12	4De	539	610	55	0.130
13	250	0.06	4De	481	363	40	0.170
14	250	0.09	4De	509	480	50	0.122
15	250	0.12	4De	536	593	60	0.127
16	300	0.06	4De	370	346	60	0.152
17	300	0.09	4De	481	466	70	0.129
18	300	0.12	4De	544	595	70	0.115
19	200	0.06	4D	305	356	80	0.076
20	200	0.09	4D	379	509	80	0.076
21	200	0.12	4D	441	652	110	0.070
22	250	0.06	4D	314	362	80	0.073
23	250	0.09	4D	353	499	105	0.059
24	250	0.12	4D	377	601	115	0.065
25	300	0.06	4D	276	364	70	0.085
26	300	0.09	4D	358	495	100	0.068
27	300	0.12	4D	378	607	120	0.077
28	200	0.06	5D	276	343	75	0.073
29	200	0.09	5D	304	470	75	0.044
30	200	0.12	5D	365	637	80	0.062
31	250	0.06	5D	273	390	55	0.060
32	250	0.09	5D	306	471	70	0.101
33	250	0.12	5D	333	606	80	0.051
34	300	0.06	5D	222	325	80	0.049
35	300	0.09	5D	299	516	90	0.063
36	300	0.12	5D	301	591	95	0.052

of the machine, premature dulling of the cutter, and deterioration of the quality of the drilled hole. As a result, it is critical to keep Fz under control [3]. The effect of drilling settings on Fz was explored in this work when drilling Al 7075-T651 material with a U drill. Table 5 shows the Fz values acquired as a result of the experiments. According to these results, the highest Fz value was produced utilizing the 4De U drill at the highest Vc and *f* values. The lowest

Fz value was reached by combining the 5D U drill with the highest Vc and the lowest f. Figure 5 is obtained by considering the experimental results. Fz increased with the increase of f for all U drills when Fig. 5 is analyzed. This outcome is consistent with the literature [3, 7]. According to the literature, when f grows, the cutter penetrates the part faster; thus, as the chip cross-section increases, chip creation becomes more difficult, and Fz increases [3]. Although it was stated in

Fig. 5 Variation of Fz depending on drilling parameters
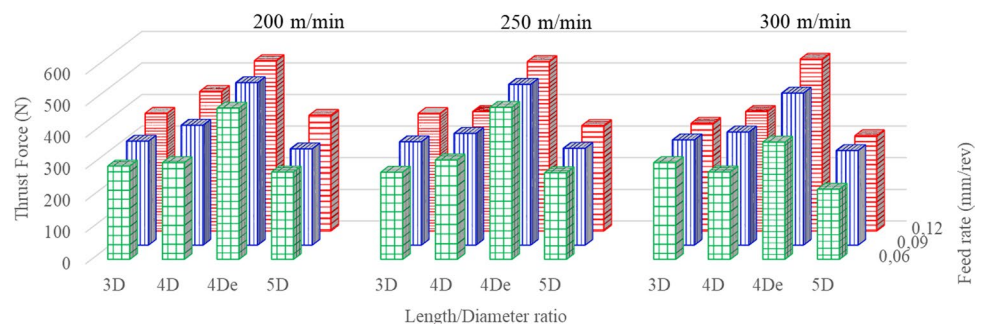
some studies that Fz decreased with the increase of Vc [4], there was no significant decrease in the current study. The values showed little variation with the increase in Vc [8]. When all Vc is averaged, the average percentage increase in Fz is 13% for 3D, 22.1% for 4D, 14.4% for 4De, and 18.9% for 5D, with a 50% rise in f from 0.06 to 0.09 mm/rev. While f grew by 33.3% from 0.09 to 0.12 mm/rev, the average percentage of Fz increase was 9.7% for 3D, 9.6% for 4D, 7.7% for 4De, and 9.9% for 5D. Table 6 displays the Anova evaluation findings for Fz with a 95% confidence interval. The R^2 value for the test was calculated at 97.6%. According to these results, the effects of drilling parameters on Fz were ranked as LD (76.45%), f (16.57%), and Vc (2.43%) according to $p < 0.05$ significance values. The LD was determined to be the most effective drilling parameter on Fz. It has also been found in similar studies that drill length and feed rate are important parameters for the thrust force [46]. It was concluded that other cutting parameters and their combinations did not have a linearly significant effect like the studies in the literature [8], since $p > 0.05$.

Considering the mean Fz according to LD, Fig. 6 is obtained. The values were calculated by taking the average of nine experiments for each U drill. The 4De U drill with the extra coolant hole produced a 39.89% higher average Fz than the 4D U drill without the extra coolant hole. Figure 6 shows that a 5D U drill produced the lowest average Fz value, while a 4De U drill produced the greatest average Fz value. Compared to the 3D U drill, the 4D U drill produced higher average Fz values, while the 5D U drill produced lower average Fz values. 4De U drill produced the highest average Fz values compared to all U drills. The highest Fz values occurring in the 4De U drill are thought to be caused by the extra coolant hole shown in Fig. 7 blocking or disrupting the chip flow produced by the central insert. In Fig. 8, there is an example of swarf clogging or adhering to the coolant hole and the chip evacuation channel. After a drilling test at Vc 300 m/min and F 0.06 mm/rev, this sample image was obtained for the 4De U drill. Even after the drilling test, there are still chips clogging or adhering
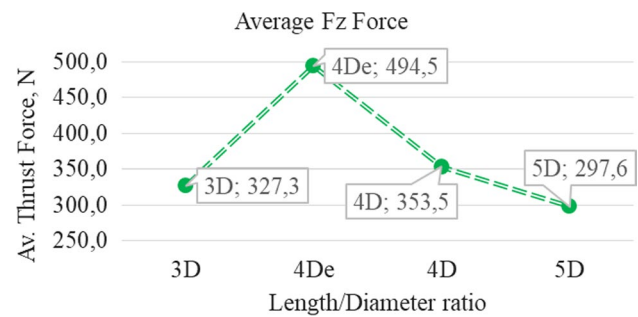

Fig. 6 Average Fz values according to LD ratio

to the coolant hole and chip evacuation channel in the part where the central insert is. The cut chips' adhesion to the drill flutes restricts the exit path of the newly removed chips, resulting in a considerable increase in Fz [4]. The influence of the extra cooling hole on the Fz force is also seen in the dynamometer's real-time force data in Fig. 9. The chips removed by the central insert may have tried to enter the coolant hole, causing the chips to clog or stick in that area and thus increase the forces. It is also understood from the graphs obtained with the dynamometer that the forces decrease once the clogged or adhering chips are freed and that this process continues with constant repetition. The shift in force along the hole axis of the cutter increases the stress on the chip, resulting in intermittent chip production [47]. The increase in intermittent chip formation causes the periodic fluctuation amplitude to increase [48]. Especially when the graphs of 4De and other U drill bodies in Fig. 9 are examined, this fluctuation in Fz is clearly seen. The extra cooling hole in 4De caused the Fz signal amplitude to differ from the others. The signal amplitudes of the other U drills other than 4De are similar. The graph in Fig. 9 shows the change in Fz values for the 1 s drilling process after each U drill bit is fully engaged in the material. The amplitude and frequency of the graph curve formed by the Fz values obtained for the 4De U drill are distinctly different from the graph curves obtained for the other U drills. For the 4De U

Table 6 Anova results for Fz

Source	DF	Seq SS	Contribution	Adj MS	f value	p value
Vc	2	6539	**2.43%**	3269.3	6.09	0.015
f	2	44,525	**16.57%**	22,262.5	41.50	0.000
LD	3	205,422	**76.45%**	68,474.0	127.65	0.000
Vc*f	4	2039	0.76%	509.8	0.95	0.469
Vc*LD	6	2536	0.94%	422.6	0.79	0.596
f*LD	6	1189	0.44%	198.2	0.37	0.885
Error	12	6437	2.40%	536.4		
Total	35	268,687	100.00%			

Bold values indicate effective drilling parameters

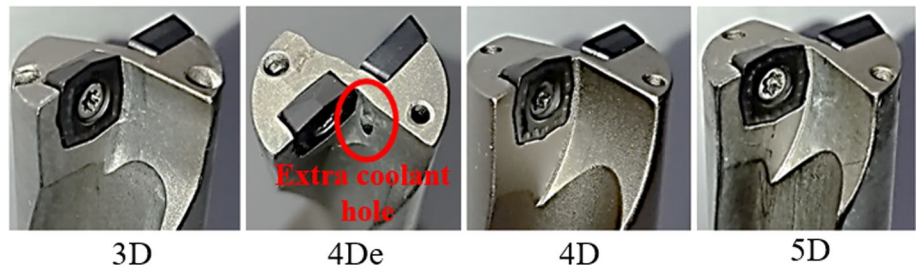**Fig. 7** Coolant holes of U drills

3D   4De   4D   5D

Fig. 8 Chips accumulated in the 4De U drill after drilling

drill, the low frequency and high amplitude are thought to be caused by chips trying to enter the coolant hole. In addition, it is stated that torque values may cause the drill to turn backwards and open the chip grooves, thus increasing the thrust forces [49]. In the current study, it is thought that the extra cooling channel in the U drill body may cause this phenomenon by creating an extra space.

3.2 Evaluation of torque

According to the findings of the current study's experiments, the highest average Mz value of 651.8 N cm was obtained at the lowest Vc and highest f values by using a 4D U drill. The smallest value, 325.44 N cm, was obtained using a 5D U drill at the largest Vc and the smallest f value. Figure 10 depicts the effect of drilling settings on Mz for all U drills as a three-dimensional graphic. According to the obtained visuals, Mz values grew as f increased for all bodies. This conclusion was also obtained in several studies published in the literature [7]. Although it was stated in some studies

Fig. 9 The first 1 s that the U drill bit is fully engaged
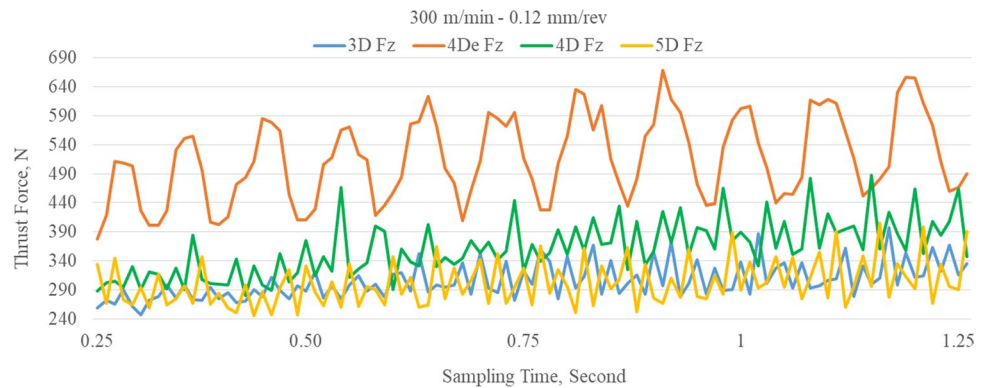
Fig. 10 Effect of drilling parameters on Mz
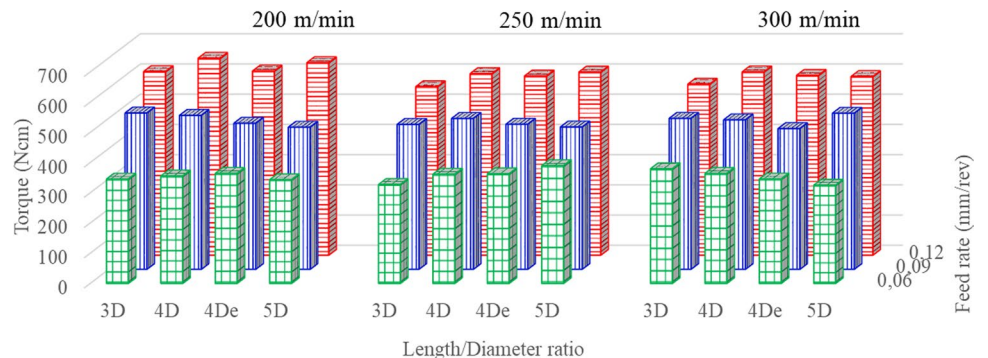
that Mz values decreased with the increase of Vc [10], a similar situation did not occur in the current study. When the Anova test results for Mz are examined, it is clear that the most effective parameter is f. The images for all U drill bodies produced very identical results. According to the Mz values calculated by taking the average of nine experiments for each U drill, the 4De U drill (477.7 N cm) with an extra coolant hole produced a 3.26% lower average Mz than the 4D U drill (493.8) without an extra coolant hole. When all Vc averages were considered, the mean percentage of Mz increase was estimated as 42.6% for 3D, 39% for 4D, 33.2% for 4De, and 38.8% for 5D, with a 50% rise in f value from 0.06 to 0.09 mm/rev. While f grew by 33.3% from 0.09 to 0.12 mm/rev, the average Mz increase percentage was found to be 15.7% for 3D, 23.7% for 4D, 25.8% for 4De, and 26.3% for 5D. An Anova test for Mz was performed at a 95% confidence interval. The R^2 value for the test was calculated at 98.84%. Calculation results are given in Table 7. According to Table 7, f was 96.04% effective on the Mz output response, according to $p < 0.05$ significance values. In accordance with the literature, the most effective cutting parameter for Mz was the input parameter f [46]. It was concluded that other cutting parameters and their combinations did not have a significant effect as $p > 0.05$. It was determined that Vc, LD, and combinations were not effective on torque since the insert positions were similar in all U drills.

The f value, which is one of the input parameters for the Anova test, has a very high effect on the Mz output response. It is clear that the LD, which is highly effective on Fz, is not effective on Mz. So different U drill sizes have no effect on Mz for drilling aluminum material. When Fig. 11 is examined, the change in Mz is seen depending on time. It can be seen that all U drill bodies fluctuate at the same rate at the start of drilling. Then, short-term, sudden increases and decreases in Mz draw attention in U drills other than 4De U drills. According to the literature, it is stated that Mz rises and falls momentarily as the chips stick to the chip evacuation channel and then break off [17]. However, if attention is paid to the Mz graph for the 4De U drill, it has consistently moved between the same Mz values from the beginning of the hole to the end. However, when looking at the graph for the other 4D U drill with the same LD ratio, instant rises and falls are remarkable. Although the extra cooling hole opened into the U drill body causes a significant increase in Fz, it can be said that it causes more stable values when Mz is taken into account. With the increase in f, sudden Mz increases are seen in the 4De U drill graph. However, these increases were not as extreme as in other U drills. The cutting speed increases as the drill moves from the center to the periphery. Since the extra coolant hole for the 4De U drill is in the center, it is thought that the clogging or adhesion of the chips has a greater effect on the Fz value but less on the Mz value. In other words, it is determined that while the chips are clogging or adhering to the chip evacuation channel where the central insert is located, less smearing occurs in the chip evacuation channel where the peripheral insert is located. Therefore, while the Fz values were higher for the 4De U drill, the Mz values were similar to the other U drills.

3.3 Evaluation of spindle load

In one aspect, the SL found on CNC machines shows how hard the spindle is forced during machining in real time. Therefore, SL provides the opportunity to determine the appropriate drilling parameters at the beginning of the work or to intervene in the drilling parameter values used during the operation of the machine. According to the results of the current study's experiments, the maximum SL value of 120% was reached utilizing the 4D U drill at the highest Vc and f values. The smallest value, 40%, was obtained at the middle Vc and the smallest f value by using a 4De U drill. According to Fig. 12, which depicts the effect of drilling parameters on SL, when f increases, SL tends to grow. The effect of increasing Vc on SL was more uncertain. According to the SL values calculated by calculating the average of nine experiments for each U drill, the 4De U drill with an extra coolant hole (56.11%) produced a 41.28% lower average SL value than the 4D U drill without an extra coolant

Table 7 Anova results for Mz

Source	DF	Seq SS	Contribution	Adj MS	f value	p value
Vc	2	1373	0.36%	686	1.87	0.196
f	2	365,359	**96.04%**	182,680	497.95	0.000
LD	3	1791	0.47%	597	1.63	0.235
Vc*f	4	2849	0.75%	712	1.94	0.168
Vc*LD	6	1927	0.51%	321	0.88	0.541
f*LD	6	2704	0.71%	451	1.23	0.357
Error	12	4402	1.16%	367		
Total	35	380,405	100.00%			

Bold value indicates effective drilling parameter
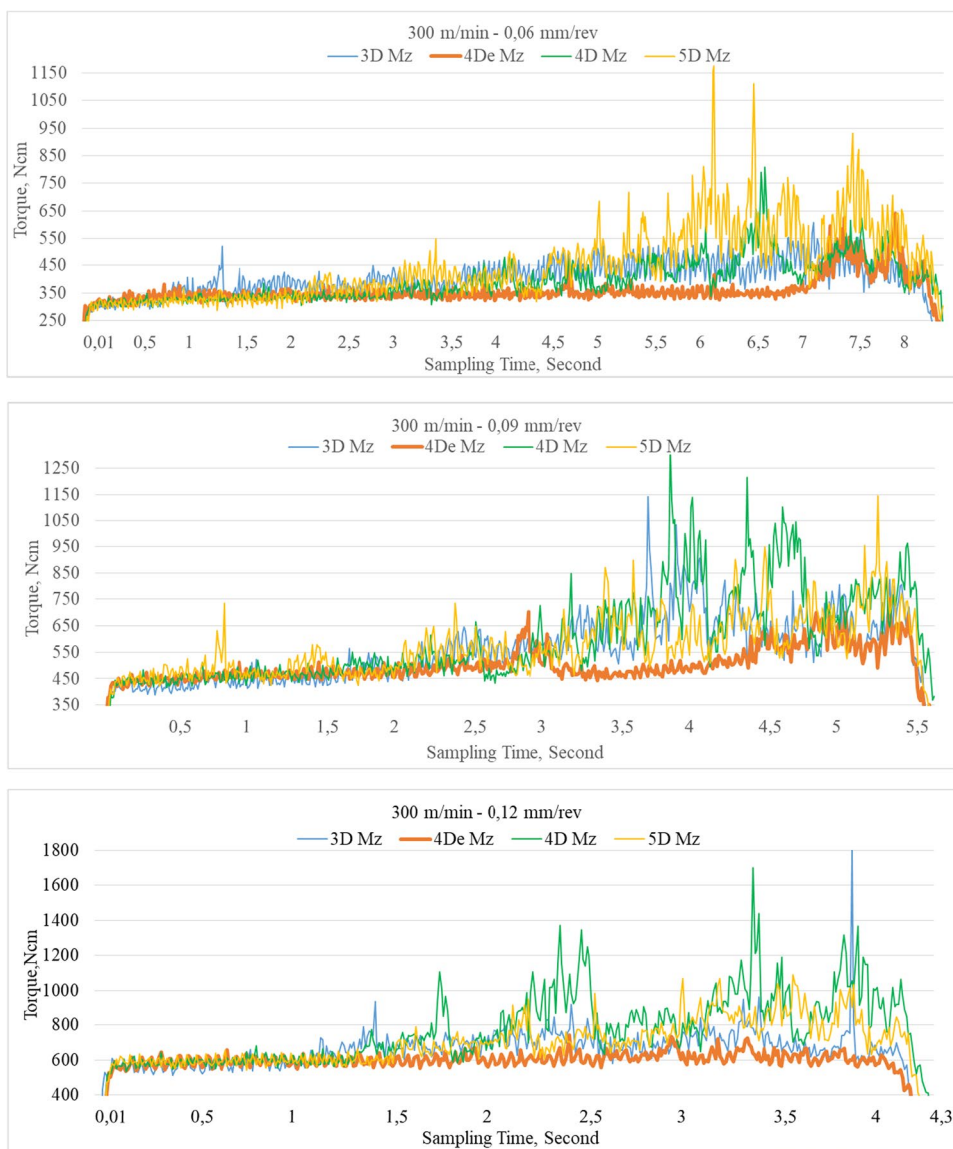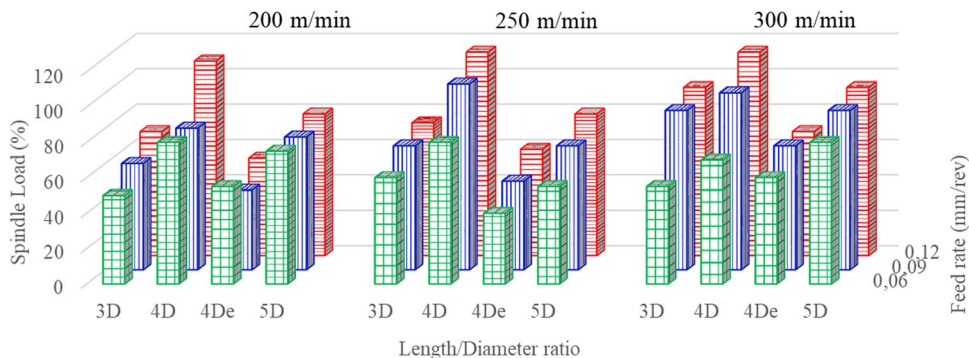
Fig. 11 Change of Mz with time

Fig. 12 Effect of drilling parameters on SL

hole (95.56%). The lowest SL was obtained with a 4De U drill. Despite a 50% increase in f from 0.06 to 0.09 mm/rev, the mean SL increase percentage in all Vc was computed as 33.4% for 3D, 24.7% for 4D, 7.8% for 4De, and 13.3% for 5D. While f grew by 33.3% from 0.09 to 0.12 mm/rev, the average SL increase percentage was 9.8% for 3D, 20.7% for 4D, 14.1% for 4De, and 8.8% for 5D. An Anova test for SL was performed at a 95% confidence interval. The R^2 value

for the test was calculated at 97.4%. Calculation results are given in Table 8. According to the significance values of $p < 0.05$ according to Table 8, LD (53.33%), f (21.27%), and Vc (8.95%) were effective on the SL output response, respectively. The most effective drilling parameter for SL was the LD ratio. Since all cutting parameters and combinations were $p < 0.05$, it was concluded that all of them had a linearly significant effect on the result. This finding is consistent with other research in the literature [50].

Considering the Mz graphics in Fig. 11 and the SL values calculated here, the drilling of Al 7075-T651 alloy with a 4De U drill resulted in a very stable result. It is interesting that while Fz values were higher for 4De, the lowest values were found for SL values. Because it is stated in various studies that higher thrust forces cause more power consumption and forced [14]. In U drills, the chip thickness acting on each insert changes due to the axial runout of the central and peripheral inserts and their geometric structure [31]. We can mention that while clogging and/or sticking occurs in the extra coolant channel in the center of the 4De U drill, less clogging or adhesion occurs in the chip evacuation channel where the peripheral insert is located. As a result of this, the cutting speed value increases as you go from the center of the drill to its circumference; we can say that it does not cause an increase in Mz since the speed is zero in the center.

3.4 Evaluation of audio signal

An audio signal is a combination of sounds from different sources. These sources consist of torsional-axial chatter, lateral chatter, rotational vibrations, coolant flow, evacuation of chips, background noises in the workshop, the noise of the spindle and gearboxes, and the noises from the hydraulic and lubrication systems of the machine tool [26]. In this study, vibration-induced audio signals were taken into account. When a cutter starts to drill a material, dominant sound waves are emitted into the environment. These sounds give us information about the dynamics of the cutting process, such as poor surface quality, dull cutting tools and loud

noise [42]. Especially the sounds that occur in U drills can tell us about vibration and its causes. In one study, it was stated that the detection of vibrations above 1000 Hz with a dynamometer was insufficient, but a microphone was a useful device for detecting chatter [43, 51]. When similar studies in the literature are examined, it has been stated that the sampling frequency of the microphone should be higher than 40 kHz in experiments using U drill [26], while higher sampling frequencies are preferred in some [52]. The influence of drilling parameters on audio signals should be investigated in this regard. Instead of evaluating the highest values in audio signal analysis, the RMS value of the signal is frequently compared [53]. x_{RMS}, which is the RMS value of an $x(n)$ signal, is calculated by considering Eq. 1. In the RMS computations, N is the number of samples [54].

$$x_{RMS} = \sqrt{\frac{1}{N} \sum_{n=1}^{N} x_n^2} \tag{1}$$

The highest SRMS value was obtained at medium Vc and the lowest f value when the 4De U drill was used, while the lowest SRMS value was obtained at middle Vc and the highest f value when the 3D U drill was used, as shown in Table 4. The effect of drilling parameters on SRMS is given in Fig. 13. According to this fig, the highest SRMS values are obtained by using the 4De U drill. The lowest values were obtained by using the 3D U drill. When the graphs are inspected, the SRMS tends to grow as f increases. On the other hand, the effect of the increase in Vc was uncertain. According to the SRMS values calculated by taking the average of nine experiments for each U drill, the 4De U drill with an extra coolant hole (0.1405 Pa) produced a 95.17% higher average SRMS value than the 4D U drill without an extra coolant hole (0.072 Pa). According to this result, it can be said that the extra cooler hole opened in the U drill causes vibration and increases the sound levels. An Anova test for SRMS was performed at a 95% confidence interval. The R^2 value for the test was calculated at 96.11%. Calculation results are given in Table 9. According to the significance
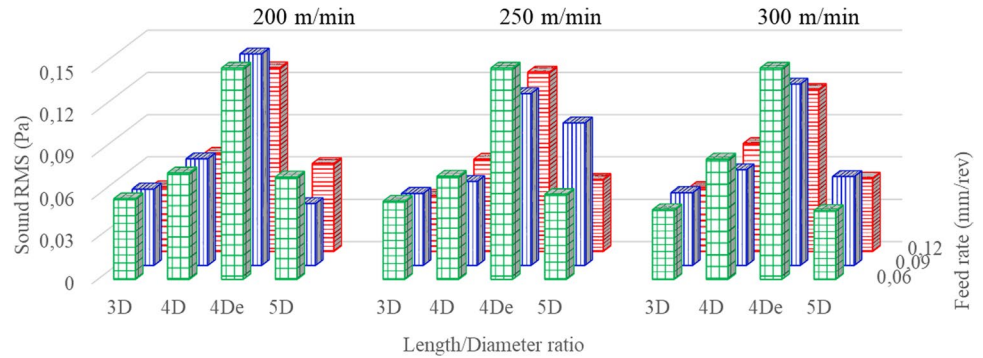
Table 8 Anova results for SL

Source	DF	Seq SS	Contribution	Adj MS	f value	p value
Vc	2	1234,7	**8,95%**	617,36	20,67	0,000
f	2	2934,7	**21,27%**	1467,36	49,14	0,000
LD	3	7358,3	**53,33%**	2452,78	82,14	0,000
Vc*f	4	502,8	**3,64%**	125,69	4,21	0,023
Vc*LD	6	637,5	**4,62%**	106,25	3,56	0,029
f*LD	6	770,8	**5,59%**	128,47	4,30	0,015
Error	12	358,3	2,60%	29,86		
Total	35	13,797,2	100,00%			

Bold values indicate effective drilling parameters

values of $p < 0.05$ according to Table 9, LD (87.53%) and f (2.89%) were effective on the SRMS output response, respectively. It was concluded that other cutting parameters and their combinations did not have a significant effect in accordance with the literature as $p > 0.05$ [55]. The most effective drilling parameter for SRMS was the LD.

As in Fig. 14, different amplitude sounds occur in the time domain with the drilling process performed by using

Fig. 13 Effect of drilling parameters on SRMS

Table 9 Anova results for SRMS

Source	DF	Seq SS	Contribution	Adj MS	f value	p value
Vc	2	0.000213	0.42%	0.000106	0.64	0.543
f	2	0.001475	**2.89%**	0.000738	4.46	0.036
LD	3	0.044671	**87.53%**	0.014890	90.00	0.000
Vc*f	4	0.000111	0.22%	0.000028	0.17	0.951
Vc*LD	6	0.000906	1.78%	0.000151	0.91	0.518
f*LD	6	0.001672	3.28%	0.000279	1.68	0.208
Error	12	0.001985	3.89%	0.000165		
Total	35	0.051035	100.00%			

Bold values indicate effective drilling parameters

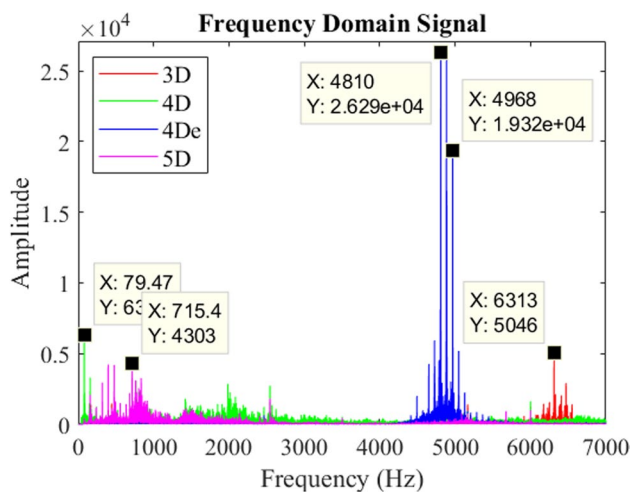**Fig. 14** Time domain representation of audio signals (300 m/min, 0.12 mm/rev)
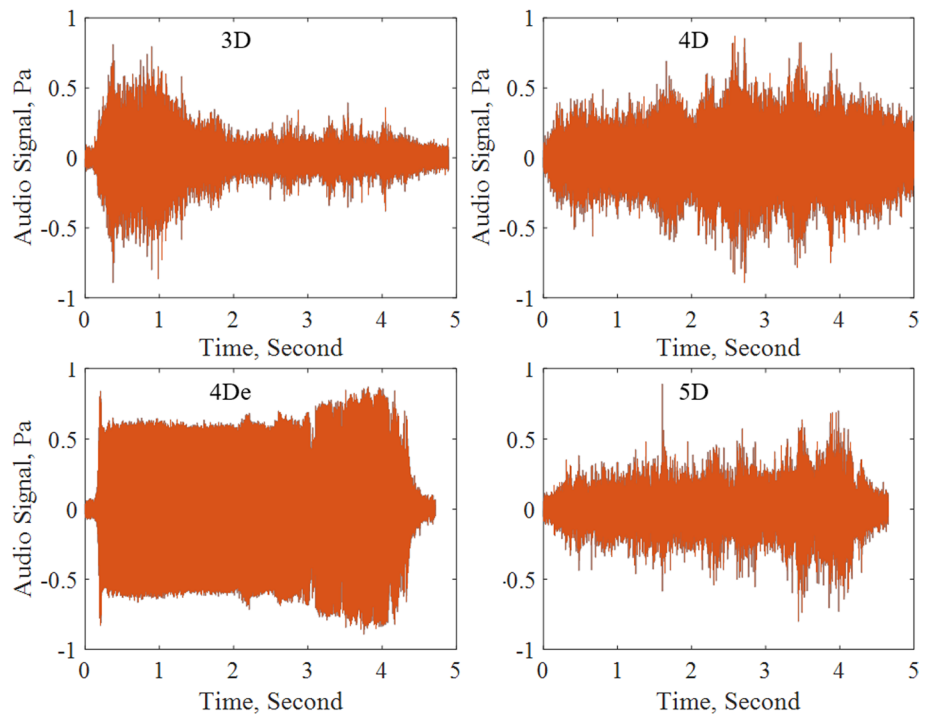
**Fig. 15** Display of audio signals in the frequency domain (300 m/min, 0.12 mm/rev)

different U drills. In order to make meaningful inferences from these data, the frequency domain is passed. Thus, vibrations produced by the use of U drills can be distinguished. For the transition to the frequency domain, the fast Fourier transform (FFT) method is used. Figure 15 depicts the frequency domain graph created as a result of the transformation in this investigation. When examining Fig. 15, 6313 Hz for 3D U drill, 79.47 Hz for 4D U drill, 4810 Hz for 4De U drill, and finally 715.4 Hz for 5D U drill are the dominant frequencies, respectively. The amplitude of the frequency obtained with the 4De U drill was very high compared to the other U drills. This means that the vibrations obtained with the 4De U drill are higher than the others. As stated in the previous sections, it can be said that the

third extra cooling hole opened in the 4De U drill body is the cause of this result. It can be said that the extra coolant hole opened on the U drill body causes more vibrations by causing dynamic instability in the drilling process. The differences in Fz and Mz caused by each insert are said to induce torsional and axial vibrations [25]. It has been stated that torsional rigidity determines how much the drill can rotate under the cutting torque, while the torsional stiffness decreases with the effect of the cooling holes drilled into the drill [56].

3.5 Insert, disc and chip images

Figure 16 shows the rake and flank faces of the central and peripheral inserts for Vc 300 m/min and f 0.12 mm/rev. Smearing occurred on the rake and flank faces of both the central and peripheral inserts as a result of drilling operations done with all U drills. When looking at the flank faces of the central inserts with 4De and 5D U drills, there are very few friction marks marked in a red circle. It is considered that this result may have occurred due to the effect of scratching [57]. Furthermore, the edge width influenced by cutting is higher on the flank sides of both the central and peripheral inserts utilized with the 4De U drill. It is thought that this result may have been achieved by the fact that the cutter was exposed to more vibration by being vulnerable to dynamic loads due to the effect of the extra cooling hole opened in the body [56]. As a result of drilling through the hole with a U drill, a disc is generated at the hole's exit. All discs were collected within the scope of this experiment. The evolution of the disk images for all U drills is similar. When the images in Fig. 17 were evaluated, the best stable cutting result was found with a 3D U drill at 200 m/min

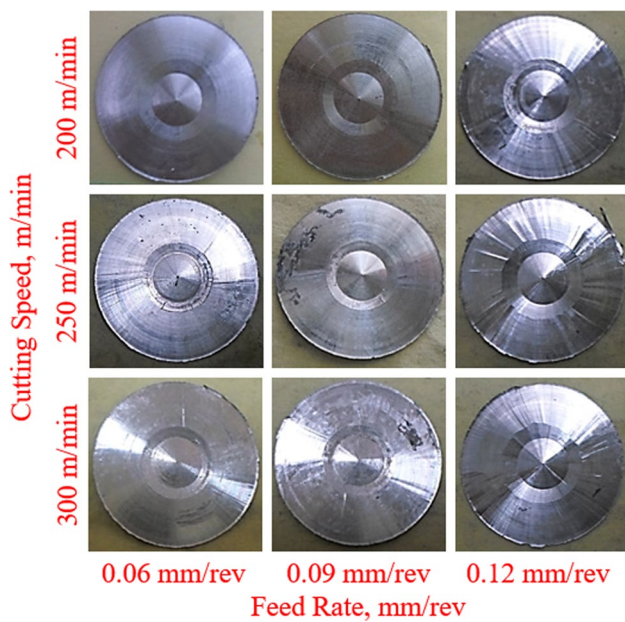**Fig. 16** Used insert images (300 m/min, 0.12 mm/rev)
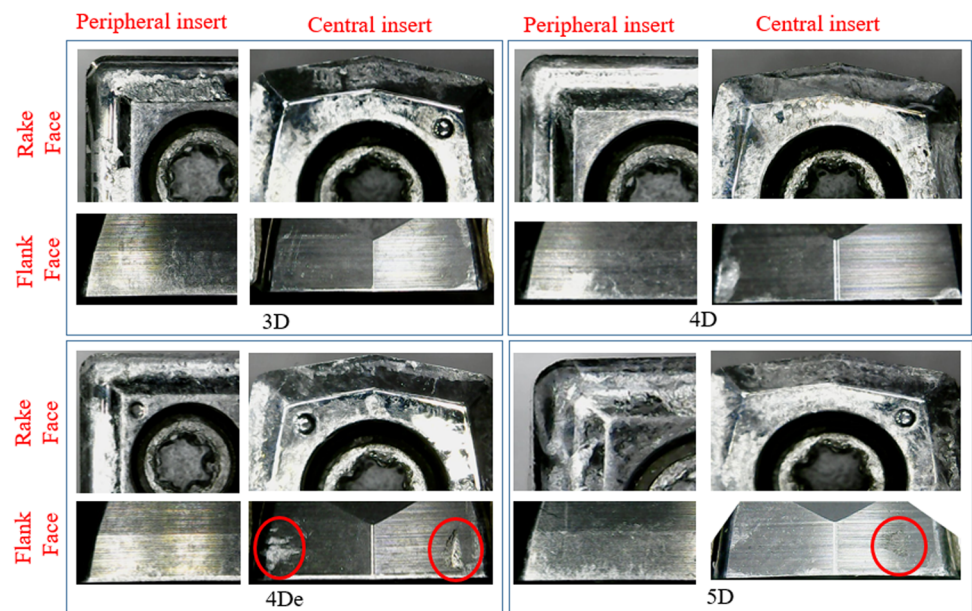
Fig. 17 Examples of disc formed by 3D U drill

and 0.06 mm/rev drilling parameters. There are no chatter marks on the disc, and it is very smooth [13]. In parallel with the increase of f, the chatter marks on the disc increase. With the increase in Vc, the chatter marks slightly changed. When Fig. 18 is examined, there is the evolution of the chips obtained during the drilling process. All of these images were obtained with a 3D U drill. Chip images obtained with other U drills are similar to these images. When the images are examined, there are typical U drill chips at 200 m/min–0.06 mm/rev. Long chips were generated by the peripheral insert, while short chips were generated by the central insert. With the increase of f, the chips became shorter and irregular. With the increase of Vc, the wavelength of the chips obtained with the peripheral insert shortened and the chips began to jam.

3.6 Multiple optimization with Taguchi based grey relational analysis

At this stage of the study, all of the output responses obtained when drilling Al 7075-T651 alloy using a U drill were optimized according to the drilling parameters. First, each output response is normalized. The "smaller is better" approach for normalization is preferred for all output responses. In

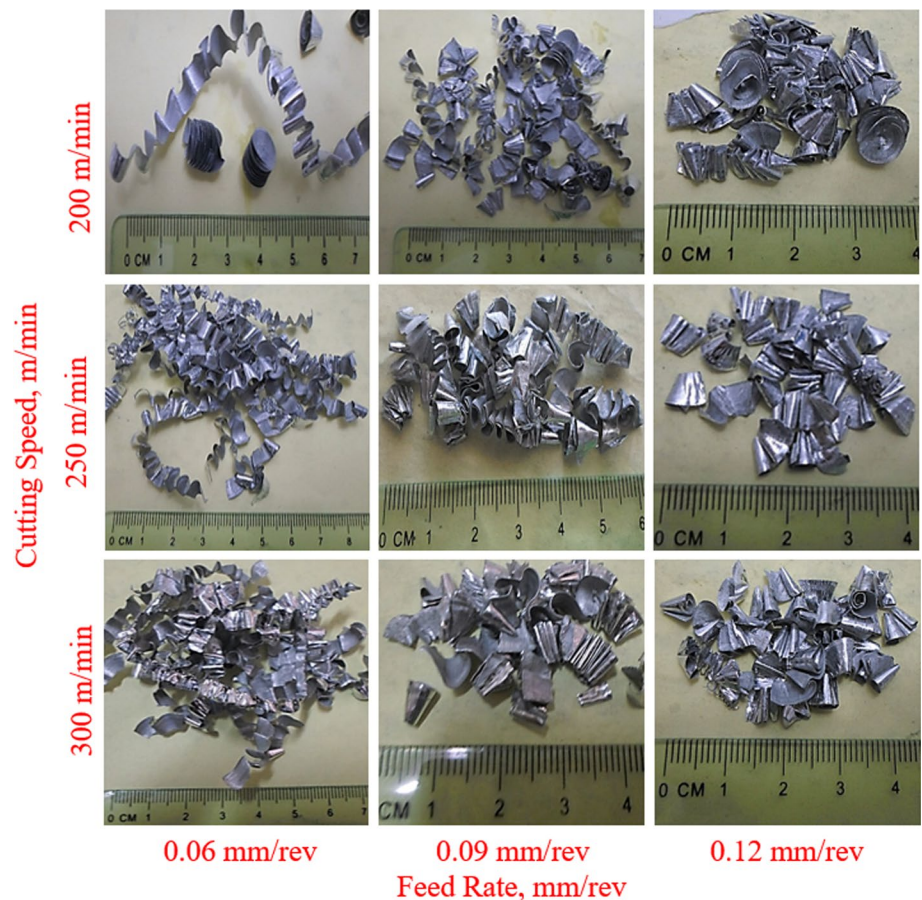**Fig. 18** Typical examples of chips cut by a 3D U drill

Table 10 Grey relational analysis results

Exp. No.	Experimental results				Normalized values				Grey relational coefficients				GRG	S/N	Order
	Fz	Mz	SL	SRMS	Fz	Mz	SL	SRMS	Fz	Mz	SL	SRMS			
1	295	345	50	0,057	0,775	0,939	0,875	0,865	0,689	0,891	0,800	0,788	0,792	−2,0252	3
2	329	517	60	0,054	0,669	0,412	0,750	0,890	0,602	0,460	0,667	0,820	0,637	−3,9177	11
3	372	608	70	0,046	0,534	0,135	0,625	0,955	0,518	0,366	0,571	0,917	0,593	−4,5377	16
4	275	328	60	0,056	0,835	0,993	0,750	0,879	0,752	0,987	0,667	0,806	0,803	−1,9071	2
5	326	479	70	0,051	0,676	0,528	0,625	0,913	0,606	0,515	0,571	0,852	0,636	−3,9296	12
6	371	558	75	0,040	0,536	0,289	0,563	1,000	0,519	0,413	0,533	1,000	0,616	−4,2052	14
7	305	380	55	0,050	0,741	0,834	0,813	0,925	0,659	0,751	0,727	0,870	0,752	−2,4785	4
8	333	500	90	0,052	0,657	0,467	0,375	0,909	0,593	0,484	0,444	0,846	0,592	−4,5549	17
9	340	566	95	0,045	0,634	0,264	0,313	0,958	0,577	0,404	0,421	0,922	0,581	−4,7141	18
10	478	364	55	0,168	0,204	0,881	0,813	0,017	0,386	0,808	0,727	0,337	0,564	−4,9673	23
11	514	483	45	0,152	0,092	0,516	0,938	0,135	0,355	0,508	0,889	0,366	0,530	−5,5205	27
12	539	610	55	0,130	0,015	0,129	0,813	0,304	0,337	0,365	0,727	0,418	0,462	−6,7125	33
13	481	363	40	0,170	0,196	0,885	1,000	0,000	0,383	0,813	1,000	0,333	0,632	−3,9807	13
14	509	480	50	0,122	0,109	0,526	0,875	0,370	0,359	0,513	0,800	0,442	0,529	−5,5343	29
15	536	593	60	0,127	0,024	0,181	0,750	0,328	0,339	0,379	0,667	0,427	0,453	−6,8829	34
16	370	346	60	0,152	0,539	0,938	0,750	0,136	0,520	0,890	0,667	0,367	0,611	−4,2830	15
17	481	466	70	0,129	0,195	0,570	0,625	0,317	0,383	0,538	0,571	0,423	0,479	−6,3970	31
18	544	595	70	0,115	0,000	0,174	0,625	0,423	0,333	0,377	0,571	0,464	0,436	−7,2007	36
19	305	356	80	0,076	0,741	0,907	0,500	0,726	0,659	0,843	0,500	0,646	0,662	−3,5832	9
20	379	509	80	0,076	0,512	0,436	0,500	0,726	0,506	0,470	0,500	0,646	0,530	−5,5071	26
21	441	652	110	0,070	0,318	0,000	0,125	0,771	0,423	0,333	0,364	0,686	0,451	−6,9082	35
22	314	362	80	0,073	0,715	0,889	0,500	0,744	0,637	0,819	0,500	0,661	0,654	−3,6863	10
23	353	499	105	0,059	0,592	0,468	0,188	0,849	0,551	0,484	0,381	0,768	0,546	−5,2539	24
24	377	601	115	0,065	0,517	0,156	0,063	0,804	0,509	0,372	0,348	0,718	0,487	−6,2541	30
25	276	364	70	0,085	0,833	0,881	0,625	0,650	0,750	0,808	0,571	0,588	0,679	−3,3570	7
26	358	495	100	0,068	0,579	0,482	0,250	0,786	0,543	0,491	0,400	0,700	0,533	−5,4588	25
27	378	607	120	0,077	0,516	0,138	0,000	0,718	0,508	0,367	0,333	0,639	0,462	−6,7066	32
28	276	343	75	0,073	0,833	0,945	0,563	0,749	0,750	0,901	0,533	0,665	0,713	−2,9435	6
29	304	470	75	0,044	0,745	0,556	0,563	0,968	0,662	0,530	0,533	0,941	0,667	−3,5232	8
30	365	637	80	0,062	0,555	0,044	0,500	0,828	0,529	0,344	0,500	0,744	0,529	−5,5296	28
31	273	390	55	0,060	0,841	0,803	0,813	0,842	0,759	0,717	0,727	0,759	0,741	−2,6074	5
32	306	471	70	0,101	0,740	0,555	0,625	0,530	0,658	0,529	0,571	0,515	0,568	−4,9083	22
33	333	606	80	0,051	0,655	0,139	0,500	0,914	0,592	0,368	0,500	0,853	0,578	−4,7609	21
34	222	325	80	0,049	1,000	1,000	0,500	0,930	1,000	1,000	0,500	0,877	0,844	−1,4699	1
35	299	516	90	0,063	0,762	0,415	0,375	0,822	0,678	0,461	0,444	0,738	0,580	−4,7285	19
36	301	591	95	0,052	0,756	0,186	0,313	0,907	0,672	0,380	0,421	0,843	0,579	−4,7450	20

the next step, the coefficients of each output response were determined and the grey relational grades (GRG) were calculated. The higher the GRG value, the closer the result of that experiment is assumed to be to the optimum result. By determining the GRG values, the optimum test sequence was determined. Table 10 shows the outcomes of the trials and computations.

Anova was estimated for the GRG values using the "bigger is better" approach. The mean value of GRG was determined using the response table for GRG in Table 11. As a result, the initial cutting condition for Vc was determined

**Table 11** Response table for GRG

Factors	Level 1	Level 2	Level 3	Level 4	Delta
Cutting speed	0.5942	0.6036	0.5941		0.010
Feed rate	0.7039	0.5689	0.5190		0.185
Length/diameter	0.6669	0.6443	0.5562	0.5217	0.145
The GRG's total mean value = 0.5972					

Table 12 Anova results for GRG

Source	DF	Seq SS	Contribution	Adj MS	f value	p Value
Vc	2	0.000716	0.19%	0.000358	0.39	0.684
f	2	0.219731	**57.52%**	0.109865	120.11	0.000
LD	3	0.130069	**34.05%**	0.043356	47.40	0.000
Vc*f	4	0.007718	2.02%	0.001929	2.11	0.142
Vc*LD	6	0.006579	1.72%	0.001096	1.20	0.370
f*LD	6	0.006214	1.63%	0.001036	1.13	0.401
Error	12	0.010976	2.87%	0.000915		
Total	35	0.382003	100.00%			

Bold values indicate effective drilling parameters

Fig. 19 Main effects plot for GRG
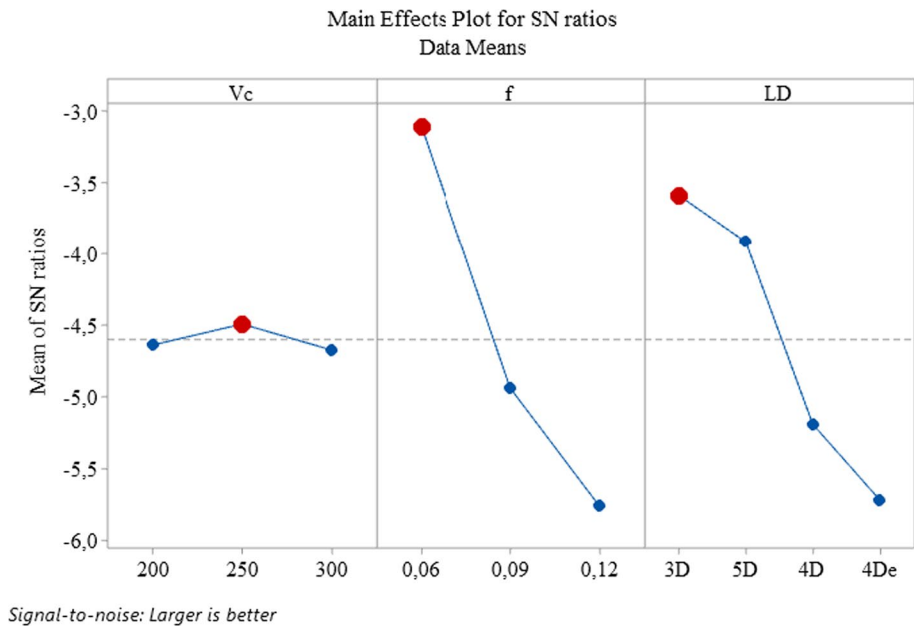
to be level 1, level 2 for f, and level 3 for LD. Table 12 displays the calculated ANOVA results. According to the 95% confidence interval Anova results, f (57.52%) and LD (34.05%) were effective on GRG. Figure 19 shows the main effects plot for GRG according to the S/N ratios. The most successful drilling settings on GRG were identified to be 3D U drill for LD, 250 m/min for Vc, and 0.06 mm/rev for f, according to this graph.

3.6.1 Verification of GRA optimization

The verification of the derived optimum parameters is the final stage of Taguchi-based grey relational analysis. Table 13 shows the outcomes of the validation studies. While the initial GRG value was 0.637, the estimation result was calculated as 0.798. The GRG value obtained as a result of the validation experiments was 0.803. Estimated and experimental results were higher than the initial cutting conditions. In addition, the correlation between the estimated and experimental results is quite high. According

Table 13 Results of validation experiments

Level	Initial cutting conditions	Optimal cutting conditions	
		Prediction	Experiment
	$Vc_1\ f_2\ LD_3$	$Vc_2\ f_1\ LD_1$	$Vc_2\ f_1\ LD_1$
Fz	329		275
Mz	517		328
SL	60		60
SRMS	0.054		0.056
GRG	0.637	0.798	0.803

Improvement in GRG = 0.166

Percentage of improvement in GRG = 26.06

to Table 13, an improvement of 0.166 was achieved in the GRG. The improvement in the percent GRG value was calculated at 26.06. In the study of Yağmur [33], 21.87% in GRG, Wang et al. [58] achieved an improvement of 13.88%. The value obtained in the GRG with the current study is quite compatible with the studies in the literature.

4 Conclusion

The effects of cutting parameters determined in this study on drilling were compared with the Fz and Mz obtained from the dynamometer, the SL from the CNC machine tool, and the RMS value of the sound information obtained with a microphone. Each output response is interpreted using the Anova test and graphs. Similarities and differences between the data were trying to be determined. Then, taking into account all output responses, optimal input factors were attempted to be discovered via multi-response optimization. For multiple response optimization, a Taguchi-based grey relational analysis method was applied. Obtained results are listed below.

1. While the ratio of length to diameter was the most effective parameter on Fz, Mz, and SRMS, the feed rate was the most effective parameter on SL. The Fz and Mz values grew as the feed rate increased. In drilling operations, it is critical to use the suitable U drill.
2. While the extra coolant hole caused an increase in Fz and SRMS values, it caused intermittent chip formation and a decrease in SL values. On the Mz, it did not cause a remarkable change due to its location close to the center. Users who want to avoid the negative effects of thrust force and excessive noise should not choose U drills with extra cooling holes.
3. When the images of the inserts as a result of the drilling process were examined, adhesion was found on the chip surfaces of almost all inserts. Considering the flank surfaces of the inserts used in the U drill with the extra coolant hole, the edge width affected by cutting is the highest. When a U drill with an extra coolant hole is used, the dynamic stiffness decreases, causing more chatter and thus an increase in the area affected by the cutting.
4. Considering the chips obtained as a result of drilling, with the increase in f value, the chip lengths were shortened and irregular, compacted chips were obtained.
5. The Anova analysis for each experimental output response revealed that the length/diameter ratio of U drills had the greatest effect on thrust force (76.45%), spindle load (53.33%), and audio signal (87.53%), but had no effect on torque.
6. The 4De U drill with the extra coolant hole produced 39.89% more thrust force, 95.17% more audio signal value, 41.28% less spindle load, and 3.26% less torque value than the 4De U drill without.
7. The calculated GRG value for the experimental output responses Fz, Mz, SL, and SRMS for the beginning parameters $Vc_1 f_2 LD_3$ is 0.637, and the predicted GRG value for the optimal drilling parameter determination

is 0.798. The GRG value of the output responses for the experimental drilling parameters $Vc_2 f_1 LD_1$ determined as a result of the applied Taguchi-based gray relational analysis was found to be 0.803. Accordingly, with the statistical optimization method applied, a 26.06% improvement was achieved in the GRG value compared to the initial parameters. As the most optimal input parameter, the LD ratio was determined to be Vc 250 m/min, f 0.06 mm/rev, and the 3D U drill.
8. As a result of optimization with Taguchi-based gray relational analysis, an improvement of 16.41% in Fz and 36.56% in Mz was achieved.

Availability of data and material The authors confirms that data supporting the findings of this study are available in the article.

Code availability No software application or custom code used.

Declarations

Conflict of interest The authors have no competing interests that are relevant to the content of this work to declare.

Ethics approval Not applicable.

Consent to participate Not applicable.

Consent for publication Not applicable.

References

1. Totten GE, MacKenzie DS (2003) Handbook of aluminum: vol. 1: physical metallurgy and processes. New York, USA
2. Committee AIH (1992) Properties and selection nonferrous alloys and special-purpose materials. ASM Int 2:1143–1144. https://doi.org/10.31399/asm.hb.v02.9781627081627
3. Yaşar N (2019) Thrust force modelling and surface roughness optimization in drilling of AA-7075: FEM and GRA. J Mech Sci Technol 33(10):4771–4781. https://doi.org/10.1007/s12206-019-0918-5
4. Paktinat H, Amini S (2017) Ultrasonic assistance in drilling: FEM analysis and experimental approaches. Int J Adv Manuf Technol 92(5):2653–2665. https://doi.org/10.1007/s00170-017-0285-2
5. Li S, Zhang D, Liu C, Tang H (2020) Exit burr height mechanistic modeling and experimental validation for low-frequency vibration-assisted drilling of aluminum 7075–T6 alloy. J Manuf Process 56:350–361. https://doi.org/10.1016/j.jmapro.2020.04.083

6. Astakhov VP (2014) Drills: science and technology of advanced operations. New York, USA

7. Luo H, Fu J, Wu T, Chen N, Li H (2021) Numerical simulation and experimental study on the drilling process of 7075–t6 aerospace aluminum alloy. Materials 14(3):553. https://doi.org/10.3390/ma14030553

8. Patel G (2021) Experimental modeling and optimization of surface quality and thrust forces in drilling of high-strength Al 7075 alloy: CRITIC and meta-heuristic algorithms. J Braz Soc Mech Sci Eng 43(5):1–21. https://doi.org/10.1007/s40430-021-02928-3

9. Kao JY, Hsu CY, Tsao CC (2019) Experimental study of inverted drilling Al-7075 alloy. Int J Adv Manuf Technol 102(9):3519–3529. https://doi.org/10.1007/s00170-019-03416-8

10. Amini S, Soleimani M, Paktinat H, Lotfi M (2017) Effect of longitudinal−torsional vibration in ultrasonic-assisted drilling. Mater Manuf Processes 32(6):616–622. https://doi.org/10.1080/10426914.2016.1198027

11. Ucun İ (2016) 3D finite element modelling of drilling process of Al7075-T6 alloy and experimental validation. J Mech Sci Technol 30(4):1843–1850. https://doi.org/10.1007/s12206-016-0341-0

12. Bagci E, Ozcelik B (2005) Analysis of temperature changes on the twist drill under different drilling conditions based on Taguchi method during dry drilling of Al 7075–T651. Int J Adv Manuf Technol 29(7):629–636. https://doi.org/10.1007/s00170-005-2569-1

13. Parsian A (2018) Regenerative chatter vibration in indexable drills: modeling and simulation. Dissertation, University West

14. Rahman M, Seah K, Venkatesh V (1988) Performance evaluation of endrills. Int J Mach Tools Manuf 28(4):341–349. https://doi.org/10.1016/0890-6955(88)90048-X

15. Rahman M, Matin M, Seah K (1993) A study of the vibrational dynamics of an endrill clamped by side-locking. J Manuf Sci Eng 115(4):438–443. https://doi.org/10.1115/1.2901787

16. Wang S, Venkatesh V, Xue W (1991) A study on modification of endrills for finishing holes. J Mater Process Technol 28(1–2):83–92. https://doi.org/10.1016/0924-0136(91)90208-V

17. Venkatesh V, Xue W (1996) A study of the built-up edge in drilling with indexable coated carbide inserts. J Mater Process Technol 58(4):379–384. https://doi.org/10.1016/0924-0136(95)02211-2

18. Heisel U, Luik M, Eisseler R, Schaal M (2005) Prediction of parameters for the burr dimensions in short-hole drilling. CIRP Ann 54(1):79–82. https://doi.org/10.1016/S0007-8506(07)60054-7

19. Tasdelen B, Wikblom T, Ekered S (2008) Studies on minimum quantity lubrication (MQL) and air cooling at drilling. J Mater Process Technol 200(1–3):339–346. https://doi.org/10.1016/j.jmatprotec.2007.09.064

20. Ahmed LS, Kumar MP (2016) Cryogenic drilling of Ti–6Al–4V alloy under liquid nitrogen cooling. Mater Manuf Processes 31(7):951–959. https://doi.org/10.1080/10426914.2015.1048475

21. Sheth S, George P (2016) Experimental investigation, prediction and optimization of cylindricity and perpendicularity during drilling of WCB material using grey relational analysis. Precis Eng 45:33–43. https://doi.org/10.1016/j.precisioneng.2016.01.002

22. Nieslony P, Cichosz P, Krolczyk G, Legutko S, Smyczek D, Kolodziej M (2016) Experimental studies of the cutting force and surface morphology of explosively clad Ti–steel plates. Measurement 78:129–137. https://doi.org/10.1016/j.measurement.2015.10.005

23. Nieslony P, Krolczyk G, Zak K, Maruda R, Legutko S (2017) Comparative assessment of the mechanical and electromagnetic surfaces of explosively clad Ti–steel plates after drilling process. Precis Eng 47:104–110. https://doi.org/10.1016/j.precisioneng.2016.07.011

24. Griffin R, Cao Y, Peng J, Chen X (2016) Tool wear monitoring and replacement for tubesheet drilling. Int J Adv Manuf Technol 86(5):2011–2020. https://doi.org/10.1007/s00170-015-8325-2

25. Parsian A, Magnevall M, Eynian M, Beno T (2017) Time domain simulation of chatter vibrations in indexable drills. Int J Adv Manuf Technol 89(1):1209–1221. https://doi.org/10.1007/s00170-016-9137-8

26. Parsian A, Magnevall M, Beno T, Eynian M (2017) Sound analysis in drilling, frequency and time domains. Procedia CIRP 58:411–415. https://doi.org/10.1016/j.procir.2017.03.242

27. Kantharaj I, Sekar M, Solomon AB, Kumar NM, Sunny KA (2019) U-drill embedded with phase change heat transfer device for machining applications. Case Stud Therm Eng 15:100533. https://doi.org/10.1016/j.csite.2019.100533

28. Svensson D, Andersson T, Andersson Lassila A (2022) Coupled Eulerian-Lagrangian simulation and experimental investigation of indexable drilling. Int J Adv Manuf Technol 121(1–2):471–486. https://doi.org/10.1007/s00170-022-09275-0

29. Heisel U, Schaal M (2009) Burr formation in short hole drilling with minimum quantity lubrication. Prod Eng Res Devel 3(2):157–163. https://doi.org/10.1007/s11740-009-0153-5

30. Biermann D, Hartmann H (2012) Reduction of burr formation in drilling using cryogenic process cooling. Procedia cIRP 3:85–90. https://doi.org/10.1016/j.procir.2012.07.016

31. Kaymakci M, Kilic Z, Altintas Y (2012) Unified cutting force model for turning, boring, drilling and milling operations. Int J Mach Tools Manuf 54:34–45. https://doi.org/10.1016/j.ijmachtools.2011.12.008

32. Kilic Z, Altintas Y (2016) Generalized mechanics and dynamics of metal cutting operations for unified simulations. Int J Mach Tools Manuf 104:1–13. https://doi.org/10.1016/j.ijmachtools.2016.01.006

33. Yağmur S (2021) The effects of cooling applications on tool life, surface quality, cutting forces, and cutting zone temperature in turning of Ni-based Inconel 625. Int J Adv Manuf Technol 116(3):821–833. https://doi.org/10.1007/s00170-021-07489-2

34. Gökçe H (2022) Modelling and optimization for thrust force, temperature and burr height in drilling of custom 450. Exp Tech 46(4):707–721. https://doi.org/10.1007/s40799-021-00510-z

35. Barik T, Pal K, Sahoo P, Patra K (2022) Sensor-based strategies for accurate prediction of drilled hole surface integrity of CFRP/Al7075 hybrid stack. Mech Adv Mater Struct. https://doi.org/10.1080/15376494.2022.2131945

36. Barik T, Pal K (2022) Prediction of TiAlN-and TiN-coated carbide tool wear in drilling of bidirectional CFRP laminates using wavelet packets of thrust–torque signatures. J Braz Soc Mech Sci Eng 44(8):364. https://doi.org/10.1007/s40430-022-03673-x

37. Zhu G, Hu S, Tang H (2021) Prediction of tool wear in CFRP drilling based on neural network with multicharacteristics and multisignal sources. Compos Adv Mater 30:1–15. https://doi.org/10.1177/2633366X20987234

38. Panda SS, Chakraborty D, Pal SK (2008) Flank wear prediction in drilling using back propagation neural network and radial basis function network. Appl Soft Comput 8(2):858–871. https://doi.org/10.1016/j.asoc.2007.07.003

39. Samavi J, Goharimanesh M, Akbari A, Dezyani E (2018) Optimisation of drilling parameters on St37 based on Taguchi method. J Braz Soc Mech Sci Eng 40:1–9. https://doi.org/10.1007/s40430-018-1245-y(0123456789(),-volV)(012345678

40. Nair U, Krishna BM, Namboothiri V, Nampoori V (2010) Permutation entropy based real-time chatter detection using audio signal in turning process. Int J Adv Manuf Technol 46(1):61–68. https://doi.org/10.1007/s00170-009-2075-y

41. Quintana G, Ciurana J, Ferrer I, Rodriguez CA (2009) Sound mapping for identification of stability lobe diagrams in milling

processes. Int J Mach Tools Manuf 49(3–4):203–211. https://doi.org/10.1016/j.ijmachtools.2008.11.008

42. Hynynen KM, Ratava J, Lindh T, Rikkonen M, Ryynänen V, Lohtander M, Varis J (2014) Chatter detection in turning processes using coherence of acceleration and audio signals. J Manuf Sci Eng 136(4):1–14. https://doi.org/10.1115/1.4026948

43. Weingaertner WL, Schroeter RB, Polli ML, de Oliveira GJ (2006) Evaluation of high-speed end-milling dynamic stability through audio signal measurements. J Mater Process Technol 179(1–3):133–138. https://doi.org/10.1016/j.jmatprotec.2006.03.075

44. Wang Z, Wagner TC, Guo C (2020) Smart machining process monitoring enabled by contextualized process profiles for synchronization. Smart Sustain Manuf Syst. https://doi.org/10.1520/SSMS20190040

45. Peña-Parás M-C, Rodríguez-Villalobos M, Romero-Cantú AG, Montemayor OE, Herrera M, Trousselle G, González J, Hugler W (2019) Optimization of milling parameters of 1018 steel and nanoparticle additive concentration in cutting fluids for enhancing multi-response characteristics. Wear 426:877–886. https://doi.org/10.1016/j.wear.2019.01.078

46. Kaplan Y, Okay Ş, Motorcu AR, Nalbant M (2014) Investigation of the effects of machining parameters on the thrust force and cutting torque in the drilling of AISI D2 and AISI D3 cold work tool steels. Indian J Eng Mater Sci 21:128–138

47. Lotfi M, Amini S (2017) Experimental and numerical study of ultrasonically-assisted drilling. Ultrasonics 75:185–193. https://doi.org/10.1016/j.ultras.2016.11.009

48. Guo Y, Mann JB (2017) Experimental evaluation of cutting kinematics and chip evacuation in drilling with low-frequency modulation-assisted machining. In: International Manufacturing Science and Engineering Conference American Society of Mechanical Engineers. https://doi.org/10.1115/MSEC2017-2886

49. Parsian A, Magnevall M, Beno T, Eynian M (2015) Time-domain modeling of torsional-axial chatter vibrations in indexable drills with low damping. The 4th International Conference on Virtual Machining Process Technology, Vancouver, Canada.

50. David-Müzel S, Bonhin EP, Ribeiro MV, Botelho EC, Alves MCdS (2020) Furfuryl resin/CNT/carbon fiber drilling, using carbide drill coated with Balinit-Helica. Mater Manuf Processes 35(10):1096–1103. https://doi.org/10.1080/10426914.2020.1765252

51. Delio T, Tlusty J, Smith S (1992) Use of audio signals for chatter detection and control. J Manuf Sci Eng 114(2):146–157. https://doi.org/10.1115/1.2899767

52. Schmitz TL (2003) Chatter recognition by a statistical evaluation of the synchronously sampled audio signal. J Sound Vib 262(3):721–730. https://doi.org/10.1016/S0022-460X(03)00119-6

53. Rajakumar IPT, Hariharan P, Srikanth I (2013) A study on monitoring the drilling of polymeric nanocomposite laminates using acoustic emission. J Compos Mater 47(14):1773–1784. https://doi.org/10.1177/0021998312451299

54. Brandt A (2011) Noise and vibration analysis: signal analysis and experimental procedures. Wiley

55. Şahinoğlu A, Güllü A (2015) CuZn39Pb3 malzemenin torna tezgâhında işlenmesinde oluşan akım, ses şiddeti, titreşim ve yüzey pürüzlülük değeri arasındaki ilişkinin incelenmesi. Politeknik Dergisi 23(3):615–624. https://doi.org/10.2339/politeknik.426106

56. Parsian A, Eynian M, Magnevall M, Beno T (2021) Minimizing the Negative effects of coolant channels on the torsional and torsional-axial stiffness of drills. Metals 11(9):1473. https://doi.org/10.3390/met11091473

57. Okada M, Asakawa N, Sentoku E, M'Saoubi R, Ueda T (2014) Cutting performance of an indexable insert drill for difficult-to-cut materials under supplied oil mist. Int J Adv Manuf Technol 72(1):475–485. https://doi.org/10.1007/s00170-014-5691-0

58. Wang Z, Li L (2021) Optimization of process parameters for surface roughness and tool wear in milling TC17 alloy using Taguchi with grey relational analysis. Adv Mech Eng 13(2):1–8. https://doi.org/10.1177/1687814021996530